Journal of Mining and Earth Sciences
Website: http://tapchi.humg.edu.vn

Impact of urbanization on land surface temperature using remote sensing and GIS: A case of Tay Ho district, Hanoi city, Vietnam

Ha Thu Thi Le [1,*], Trung Van Nguyen [1], Lan Thi Pham [1], Le Thi Le [2], Huong Thuy Duong [1], Long Huu Nguyen [3]

[1] *Faculty of Geomatics and Land Administration, Hanoi University of Mining and Geology, Vietnam*
[2] *Thanh Hoa University of Culture, Sports and Tourism, Vietnam*
[3] *Dong Thap University, Vietnam*

ARTICLE INFO

Article history:
Received 3rd Jan 2019
Accepted 18th Mar 2019
Available online 30th June 2019

Keywords:
Urbanization
Land surface temperature
Landsat data
GIS spatial analysis
Tay Ho district.

ABSTRACT

For over a century, the history of Hanoi has been connected to its urbanization process. This urban expansion is leading to the replacement of natural surfaces by various artificial materials. This situation has a critical impact on the environment due to the alteration of heat energy balance. This research reports an investigation into the application of remote sensing, geographic information systems (GIS) to provide information on the impact of urbanization on land surface temperature. The results show that low land surface temperature correlates positively with the coverage percentage of water and vegetation. This association is negative for built-up and dry barren of land use types. Hence, also from the results, it can be said that with an increase of built-up area, land surface temperature also increases. Especially as, where the surface is the plant or water becomes impervious, the temperature rises dramatically, from 3 to 7 degree. This information can be used by the municipal authorities and decision makers as input during urban and environmental planning.

1. Introduction

Urbanization, the conversion of other types of land to uses associated with the growth of populations and economy, is the main type of land use and land cover change in human history. Changes in land cover include changes in biotic diversity, actual and potential primary productivity, soil quality runoff, and sedimentation rates (Steven et al., 1992), and cannot be well understood without the knowledge of land use change that drives them. Therefore, land use and land cover changes have environmental implications at local and regional levels and perhaps are linked to the global

*Corresponding author
E-mail: lethithuha@humg.edu.vn

environmental process (Weng et al., 1999). Urbanization has a great impact on the climate. By covering with buildings, roads, and other impervious surfaces, urban areas generally have a higher solar radiation absorption, and greater thermal capacity and conductivity, so that heat is stored during the day and released by night. Therefore, urban areas tend to experience a relatively higher temperature compared with the surrounding rural areas. This thermal difference, in conjunction with waste heat released from urban houses, transportation, and industry, contribute to the development of urban heat.

The land surface is a complex feature that can be described as a combination of green vegetation, water surfaces, impervious surface materials, and exposed soils. As a result of this complexity, land surface temperature (LST) varies spatially and temporally. Impervious surface differs considerably between urban and suburban areas, and it is the main contributor to the surface urban heat island (SUHI) effect (Mallick et al., 2008). The growth and strength of the heat island areas during this time bring challenges for energy, the health of urban residents, water supplies, urban infrastructure and social comfort (Rhinane et al., 2012). In addition, it exacerbates heat waves and creates a negative effect on life expectancy on urban inhabitants (EPA, 2008). Typically, the average surface emissivity in urban areas is about 2% lower than the typical rural areas (Howard L., 1820). Without emissivity correction and neglecting these difference temperature retrievals of urban-rural environments can show differences of 1.5o C or more. Therefore, urban heat island effects can typically be estimated. Remote sensing and geographic information systems (GIS) has been widely applied and been recognized as a powerful and effective tool in detecting urban land use and land cover change (Ehlers et al., 1990; Treitz et al., 1992; Harris and Ventura, 1995). Satellite remote sensing collects multi-spectral, multi-resolution, multi-temporal data, and turns them into information valuable for understanding and monitoring urban land processes and for building urban land cover datasets. GIS technology provides a flexible environment for entering, analyzing and displaying digital data from various sources necessary for urban feature identification, change detection, and database development. However, a few of the urban growth studies have linked to post-change detection environmental impact analysis. The question of how to develop an operational procedure using the existing techniques of remote sensing and GIS for examining environmental impacts of rapid urban growth remains to be answered.

The relationship between land surface temperature and land cover has been documented in many studies. The correlation between surface temperature in Mexicali (Mexico) and land use was found by using remote sensing data (Cueto et. al., 2007). The relationship between land surface temperature using the thermal infrared band (band 6) and land cover changes in Zhengzhou city (Huabei Plain) using multi-temporal satellite data was analyzed by Cai et al., (2017). An algorithm to estimate the statistical correlation between land surface temperature and vegetation index was proposed by Hyung Moo Kim et al., (2005).

Many studies have used remote sensing data to determine and monitor land surface temperature distribution. The thermal infrared bands of Landsat 5 TM (band 6) and Landsat 7 ETM+ (band 61 and band 62) data were used to estimate land surface temperature in urban area (Alipour et al., 2007; Mallick et al., 2008; Kumar et al., 2012; Grishchenko, 2012; Tran et al., 2009; Trinh, 2014). The results of these studies have demonstrated that in the big cities, urban heat island effect is becoming a problem due to increasing coverage of land with impervious surfaces.

The goal of this paper is to demonstrate the integrated use of remote sensing and GIS in addressing environmental issues in Vietnam at a local level. Especially, objectives are to evaluate urban growth patterns in the Tay Ho district, Hanoi city and to analyze the impact of the urban growth on surface temperature.

2. Study area

Tay Ho district located in the Northwest of Hanoi, the capital of Vietnam has been identified as a service - tourist and cultural center and a protected area of natural landscape of the capital, Hanoi. The total area is about 24 km2 consists of

eight wards: Buoi, Nhat Tan, Phu Thuong, Quang An, Thuy Khue, Tu Lien, Xuan La, and Yen Phu.

Tay Ho district is adjacent to four districts: Long Bien district (to the east), Bac Tu Liem district (to the west), Ba Dinh district (to the south), and Dong Anh district (to the north). Tay Ho district has the largest freshwater lake of Hanoi, with more than 500 hectares of natural water and dozens of hectares of green space, Tay Ho has a fresh cool, healthful atmosphere (Fig.1).

3. Data and methodology

3.1. Data sources

Landsat data were used for this study. Two landsat data selected to classify land cover of

Figure 1. Study area in Tay Ho district, Hanoi city.

study area consist of a Landsat-5 TM data acquired on December 9th, 2004 and a Landsat-5 TM data acquired on November 8th, 2010 (download free at http://glovis.usgs.gov). The details of Landsat data were described in Table 1.

Table 1. Characteristics of satellite data used in study area.

Sensor	Spatial resolution	Processing Level	Acquired Date
TM	30 m	2A	9/12/2004
TM	30m	2A	8/11/2010

3.2. Urban expansion detection and analysis

Land cover maps of Tay Ho in 2004 and 2010 were classified from two LANDSAT 5 TM images acquired in the aforementioned years. An object-oriented approach was used for improving data classification technique. The complex objects are assigned to class hierarchy by generating decision trees. The results using many complex datasets provide better accuracy compared to traditional classification techniques (Waiyamai et al., 2004). However, the application of such a classification method for monitoring the changes of land cover in urban area was not found in the literature. This approach was used to produce a land cover map with four classes: impervious surface, water, vegetation, and barren land. The process of the object based image classification can be split into three steps: 1-segmentation; 2-classification; 3-accuracy assessment.

Firstly, the multi-resolution (MR) segmentation algorithms in eCoginition Developer 8.7 software has used in our study. Parameters for the segmentation include scale, shape ratio, and compactness/smoothness ratio was examined at different values. "Scale" is one of the important criteria in the segmentation process. Scale value directly affects the size of the segmentation objects (Trimble, 2011). Shape ratio value refers to the form and the structure of individual objects. The change in the shape ratio optimizes the spectral or spatial homogeneity of the resulting segmentation. While "smoothness" is defined as the ratio of an object's perimeter to the perimeter of this object's boundaries that run parallel to the image borders; "compactness" is the ratio of an object's perimeter to the square root of the number of pixels within that image object. We hereby chose this segmentation as the most appropriate for the purpose of our work. In segmenting these images, the spatial and spectral characteristics of the image pixels were considered. The segmentation of this study were conducted at a scale of 10, color/shape ratio (0.8/0.2), and compactness/smoothness ratio (0.5/0.5).

The second step in the object-oriented method was to classify image objects. The classification stage was done using the segmented image in association with the training data (class signatures) to achieve a good classification of the land cover pattern of the study area. The water in these categories is the most different in spectral with others, especially in near-infrared channel. Therefore, water was extracted based on band 3 and band 5 of Landsat TM. After that, the Normalized Difference Vegetation Index (NDVI), Normalized Difference Built-up Index (NDBI) were used to establish a high-quality rule-set for vegetation and impervious surface. Information on image bands, image reflectance, and the relationships between neighboring objects is required to develop a highly accurate rule-set. To improve the accuracy of the classification, manual editing was carried out.

Finally, to assess the accuracy of the classified maps, the ground truth data was used. The classification accuracy is achieved by comparing the ground truth data points with the classified images, points were sampled along roads, focusing on typical land-cover types in the region. The degree of agreement of the classified image position and the ground truth data points provides the classification accuracy of the image classification process. The accuracy of the resulting maps is based on 98 ground control points taken from high-resolution Google Earth images and fieldwork. The Kappa coefficient, which is calculated according to the Congalton's formula (Congalton, 1991), deals with the experiment between the remote sensing data and the in-situ observation.

3.3. Method of determining surface temperature from the infrared thermal images

To calculate land surface temperature, in the first step, Landsat 5 TM band data must be converted to TOA spectral radiance using the

radiance rescaling factors provided in the metadata file (LANDSAT Conversion to Radiance, Reflectance, and At-Satellite Brightness Temperature):

$$L_\lambda = M_L Q_{cal} + A_L \quad (1)$$

where: L_λ - TOA spectral radiance (Watts/(m2 * srad * μm)); M_L - Band-specific multiplicative rescaling factor from the metadata (RADIANCE_MULT_BAND_x, where x is the band number); A_L - Band-specific additive rescaling factor from the metadata (RADIANCE_ADD_ BAND_x, where x is the band number); Q_{cal} - Quantized and calibrated standard product pixel values (DN).

Table 2. LANDSAT 5 TM spectral radiance ML, AL dynamic ranges.

No.	Data type	Band	M_L	A_L
1	LANDSAT 5 TM	6	$0.055.10^{-4}$	1.18243

(Note that M_L and A_L are derived from the metadata of Landsat 5 TM data).

In the second step, the LANDSAT thermal band data can be converted from spectral radiance to brightness temperature using the following equation (LANDSAT Conversion to Radiance, Reflectance and At-Satellite Brightness Temperature):

$$T = \frac{K_2}{ln(\frac{K_1}{L_\lambda}+1)} \quad (2)$$

where: T - At satellite brightness temperature (K); K_1 - Calibration constant 1 [W/(m².sr.μm)]; K_2 - Calibration constant 2 [K].

Table 3. LANDSAT 8 thermal band calibration constants.

No.	Data type	Band	K_1 (W/ (m².sr.μm))	K_2 (Kelvin)
1	LANDSAT 5 TM	6	607.66	1260.56

For determining land surface temperature from Landsat data, land surface temperature can be calculated by the following equation (Grishchenko, 2012; Trinh, 2014; Kumar, 2012):

$$LST = \frac{T}{1+(\frac{\lambda.T}{\rho}).ln\varepsilon} \quad (3)$$

where: T - brightness temperature (K^0), λ - wavelength (11,5 μm); ε - land surface emissivity, $\rho = \frac{h.c}{\sigma}$, h - Plank's constant ($6,626.10^{-34}$ J.sec), c - velocity of light ($2,998.10^8$ m/sec), σ - Stefan Boltzmann's constant, which is equal to $5,67.10^{-8}$ $Wm^{-2}K^{-4}$.

4. Results anddiscussion

4.1. Urban expansion in Tay Ho district from 2004 to 2010

According to the accuracy assessment results of classified maps, the overall accuracy for Landsat 5 TM 2004 and Landsat 5 TM 2010 was 84.44% and 89.03% respectively; the Kappa Coefficient of those maps reached 0.81 and 0.84, respectively. The land cover maps of study area were generated in Figure 2, and land cover classes area and percentage were summarized in Table 4 and Table 5. Based on Figure 2, vegetation, water

Table 4. Structure of land cover in 2004.

Landcover / Wards	Impervious		Vegetation		Water		Bare land		Total
	Area (ha)	Area ratio (%)	Area (ha)	Area ratio (%)	Area (ha)	Area ratio (%)	Area (ha)	Area ratio (%)	Area (ha)
PhuThuong	141.39	22.48%	303.75	48.30%	150.48	23.93%	33.21	5.28%	628.83
Buoi	74.16	46.34%	6.03	3.77%	79.47	49.66%	0.36	0.22%	160.02
Nhat Tan	115.83	33.85%	108	31.56%	64.8	18.94%	53.55	15.65%	342.18
Quang An	94.86	24.12%	60.39	15.36%	233.01	59.26%	4.95	1.26%	393.21
Tu Lien	70.47	26.54%	145.98	54.98%	36.36	13.69%	12.69	4.78%	265.5
Xuan La	83.43	33.94%	136.89	55.69%	18.99	7.73%	6.48	2.64%	245.79
Yen Phu	66.33	43.28%	28.89	18.85%	53.19	34.70%	4.86	3.17%	153.27
ThuyKhue	53.73	30.37%	5.04	2.85%	117.63	66.48%	0.54	0.31%	176.94

Table 5. Structure of land cover in 2010.

Landcover / Wards	Impervious		Vegetation		Water		Bare land		Total
	Area (ha)	Area ratio (%)	Area (ha)	Area ratio (%)	Area (ha)	Area ratio (%)	Area (ha)	Area ratio (%)	Area (ha)
PhuThuong	215.28	34.24%	210.69	33.51%	164.88	26.22%	37.98	6.04%	628.83
Buoi	79.29	49.55%	1.44	0.90%	79.11	49.44%	0.18	0.11%	160.02
Nhat Tan	161.82	47.29%	79.2	23.15%	85.86	25.09%	15.3	4.47%	342.18
Quang An	131.58	33.46%	27.45	6.98%	231.93	58.98%	2.25	0.57%	393.21
Tu Lien	110.34	41.56%	123.84	46.64%	5.85	2.20%	25.47	9.59%	265.5
Xuan La	112.59	45.81%	110.25	44.86%	16.83	6.85%	6.12	2.49%	245.79
Yen Phu	82.35	53.73%	19.98	13.04%	49.23	32.12%	1.71	1.12%	153.27
ThuyKhue	58.68	33.16%	0.63	0.36%	117.54	66.43%	0.09	0.05%	176.94

Table 6. Matrices of land cover changes in Tayho district.

2004 \ 2010	Impervious (ha)	Vegetation (ha)	Water (ha)	Bare land (ha)	Total (ha)
Impervious	700.2	0	0	0	700.2
Vegetation	197.29	546.21	25.92	35.55	818.97
Water	20.43	10.71	697.23	25.56	753.23
Bare land	64.01	16.56	28.08	27.99	127.64
Total	981.93	573.48	751.23	89.1	2400.04

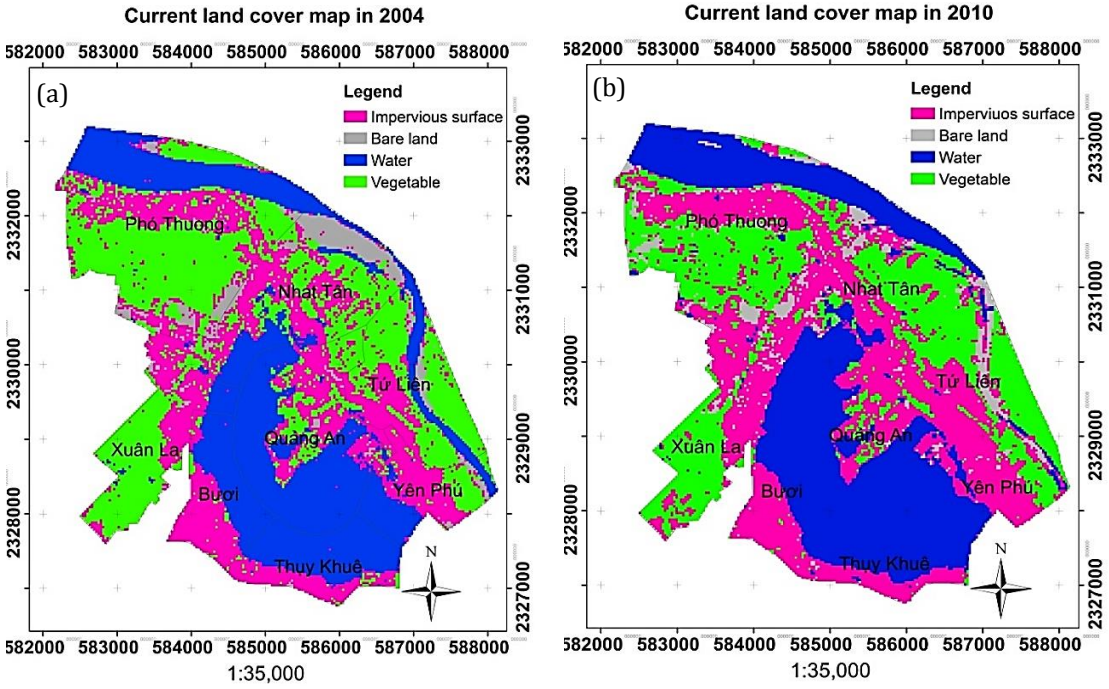

Figure 2. Spatial distribution of land cover in 2004 (a) and 2010(b).

and impervious areas were the dominant LULC classes in spatial distribution pattern. Accordingly, vegetation, water, and impervious areas were counted for about 34.1%, 31.4% and 29.1% of the total area in 2004, respectively. Meanwhile impervious, water and vegetation areas were occupied 40.9%, 31.1% and 23.8% of the total area in 2010, respectively. The vegetation, water and bare land change to impervious were about 197.19 ha, 20.43 ha and

64.01 ha of the total region study between 2004 and 2010, respectively (Table 6). The results also showed that the water surface area from 2004 to 2010 is nearly no change.

4.2. Spatial distribution of surface radiant temperature in the Tay Ho district, Hanoi City

Figure 3 and Figure 4 show the results of surface temperature distribution across the Ho Tay district. Observation maps show the lowest and highest surface temperature during study period ranges from 18.6°C to 27.2°C, and from 20.5°C to 30.6°C in 2004 and 2010, respectively. In particular, the construction of high density has the largest land surface temperature with an average value is 30°C and are shown in red on the map in 2010; concentrated in the urban areas. In contrast, the water surface and the green area of vegetation remaining lower temperatures. Particularly, the surface temperature of the water surface is the lowest, with average values reaching 18°C and is shown in dark green on the map (Figure 3). The results also show that the temperature in vegetated areas was lower in comparison with the built-up area. Because vegetation has the capability of evaporating, which help to accelerate the process of heat transfer between land surface and atmosphere. Meanwhile, the temperature in urban area covered by impervious surfaces was higher due to its construction materials shown a tendency in absorbing and holding heat, and less evaporating.

4.3. Urbanization impact on surface temperature

Table 7. Summary temperature results for the land cover of Tay Ho district between 2004 and 2010.

Wards	Temperature in 2004 (°C)			Temperature in 2010 (°C)		
	Min	Max	average	Min	Max	average
Buoi	18.6	21.8	20.2	20.9	26.7	23.6
Nhat Tan	18.6	27.1	22.0	19.3	28.0	22.7
PhuThuong	19.5	24.5	21.1	21.3	28.9	24.4
Quang An	18.6	24.0	19.9	20.9	28.0	23.2
ThuyKhue	18.6	23.2	19.9	20.4	26.7	22.7
Tu Lien	19.5	24.0	21.6	23.6	30.6	25.8
Xuan La	19.0	23.2	20.5	21.3	28.0	25.1
Yen Phu	19.0	23.6	21.0	20.9	28.0	24.7

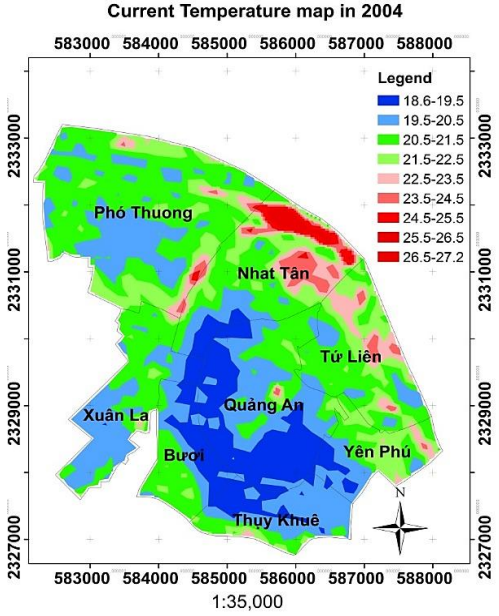

Figure 3. Spatial distribution of surface radiant temperature in 2004

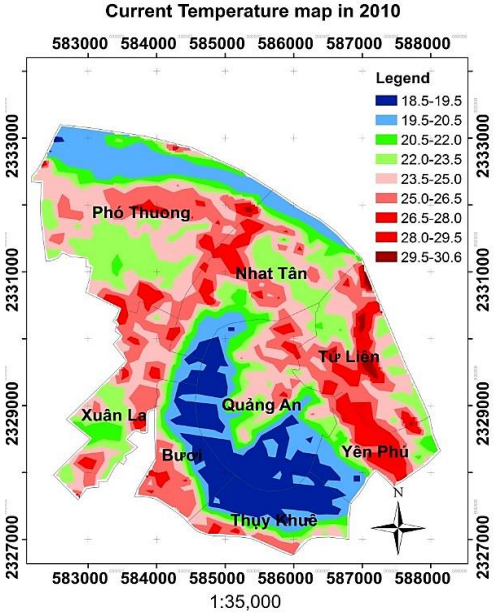

Figure 4. Spatial distribution of surface radiant temperature in 2010.

Figure 5, Figure 6, Figure7, and Figure 8 shows the relationship between the change of land cover and surface radiant temperature from 2004 to 2010. For the surface is not permeable, the temperature rises, especially at the point in which the vegetation or water becomes impervious surface as the following.

- For Buoi and Thuy Khue: the temperature increased highest, from 3^0C to 7^0C due to the vegetation gradually turning into the impervious surface.

- For Xuan La and Phu Thuong wards: the average land surface temperature increases from 2^0C to 5^0C.

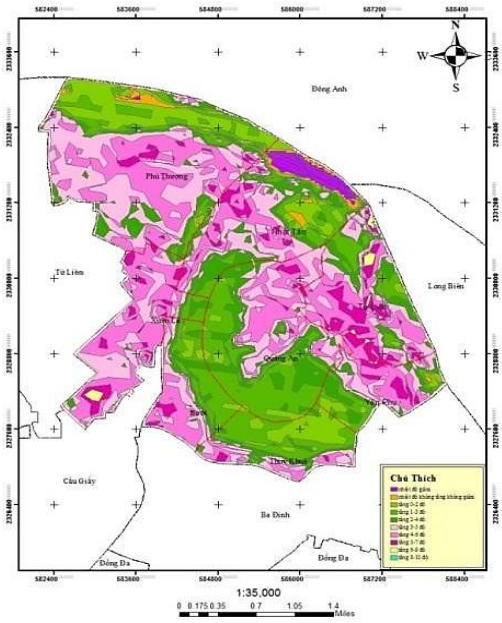

Figure 5. Change of spatial surface radiant temperature in 2004 - 2010.

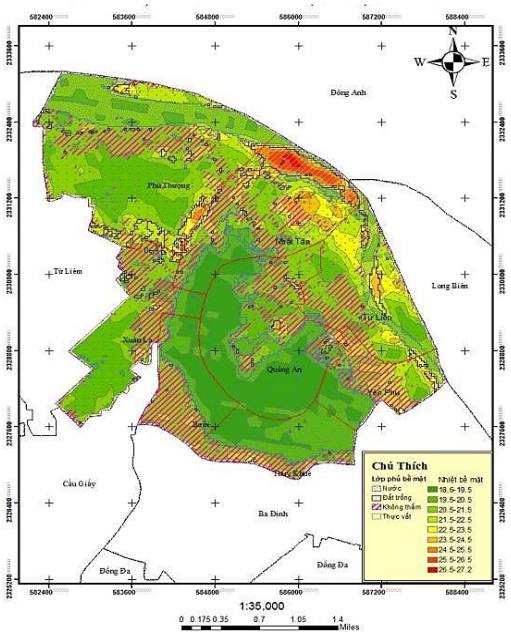

Figure 6. Spatial relationship between land cover and surface radiant temperature in 2004.

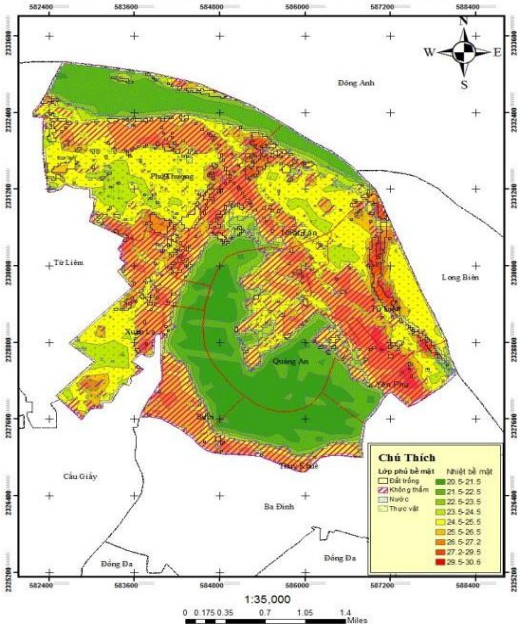

Figure 7. Spatial relationship between land cover and surface radiant temperature in 2010.

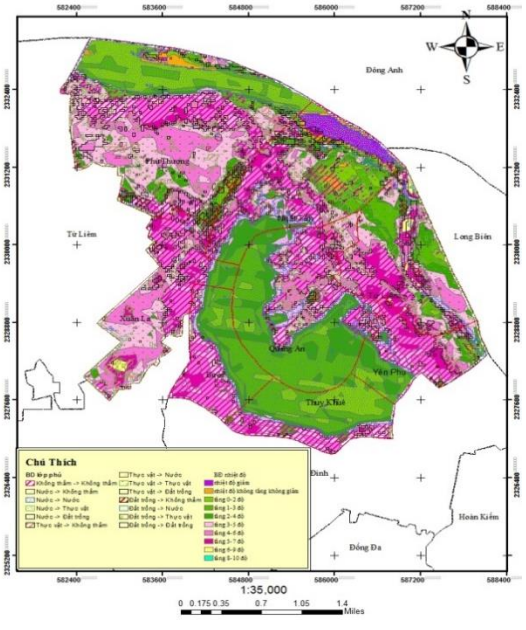

Figure 8. Spatial relationship between change in landcover and surface radiant temperature from 2004 to 2010.

- For Yen Phu and Quang An wards: the average land surface temperature increases from 1^0C to 4^0C.

- For Nhat Tan ward: the average land surface temperature between 2004 and 2010 was the same.

5. Conclusion

Identification of factors affecting the land surface temperature in urban areas is very important. Because the temperature of cities was higher than the countryside and this phenomena is due to an increase in land surface temperature and thereby creating urban heat islands has happened. The main cause of increase in urban land surface temperature is change in the structure of the Earth's surface or the so-called change of land use/land cover in these areas. The increment of land surface temperature in the long-term causes a lot of damage to the urban environment and its inhabitants as well. By identifying effective land use at land surface temperature, better urban planning can be done for urban development and partly can prevent from increasing temperatures and heat island phenomenon in urban areas.

In this study, an integrated approach of remote sensing and GIS was developed for evaluation of rapid urban expansion and its impact on surface temperature in the Tayho district, Ha Noi city, Viet Nam. Results revealed a notable increase in urban land use/cover between 2004 and 2010. The increase of surface radiant temperature was related to the decrease of biomass. The spatial pattern of radiant temperature increase was correlated with the pattern of urban expansion.

The integration of remote sensing and GIS provides an efficient way to detect urban expansion and to evaluate its impact on surface temperature. The environmental impacts of land use and land cover change can be modeled at the local level using the integrated approach of remote sensing and GIS. This methodology should be possible to apply to other regions in Vietnam or other nations that occurs rapid urbanization.

References

Alipour, T., Sarajian, M. R., Esmaseily, A., 2004. Land surface temperature estimation from thermal band of LANDSAT sensor, case study: Alashtar city. *The International Archives of the Photogrammetry. Remote Sensing and Spatial Information Sciences* 38(4). C7.

Azad, R., Heiko, B., Claire, S., John, R., Bashir, A., José, A. S., Manat, S., Qihao, W., 2017. A Review on Remote Sensing of Urban Heat and Cool Islands. *Land 2017, 6, 38. doi:10.*

Cai, Q., Ki, E., Jiang, R., 2017. Analysis of the relationship between land surface temperature and land cover changes using multi-temporal satellite data. *Nature Environment and Pollution Technology* 16(4). 1035 - 1042.

Congalton, R. G., 1991, A review of assessing the accuracy of classifications of remotely sensed data, *Remote Sensing and Environment* 37. 35 - 46.

Cueto, G., Jauregui, O. E., Toudert, D., Tejeda, M. A., 2007. Detection of the urban heat island in Mexicali and its relationship with land use. *Atmosfera* 20(2). 111 - 131.

Ehlers, M., Jadkowski, M. A., Howard, R. R., and Brostuen, D. E., 1990. Application of A remote sensing-GIS evaluation of urban expansion 2013 SPOT data for regional growth analysis and local planning. *Photogrammetric Engineering and Remote Sensing* 56. 175 - 180.

EPA, 2008. Reducing Urban Heat Islands: Compendium of Strategies Urban Heat Island Basics.

Grishchenko, M. Y., 2012. ETM+ thermal infrared imagery application for Moscow urban heat island study. *Current Problems in Remote Sensing of the Earth from Space* 9(4). 95 - 101. (In Russian).

Harris, P. M., and Ventura, S. J., 1995, The integration of geographic data with remotely sensed imagery to improve classiŽcation in an urban area. *Photogrammetric Engineering and Remote Sensing* 61. 993 - 998.

Hassan, R., Atika H., Hicham, B., Aziza, B., 2012. Contribution of Landsat TM Data for the Detection of Urban Heat Islands Areas Case of

Casablanca. *Journal of Geographic Information System.*

Hyung, M. K., Beob, K. K., Kang, S. Y., 2005. A statistic correlation analysis algorithm between land surface temperature and vegetation index. *International Journal of Information Processing Systems* 1(1). 102 - 106.

Javed, M., Yogesh, K. and Bharath, B. D., 2008. Estimation of land surface temperature over Delhi using Landsat 7 ETM+. *J. Ind. Geophys. Union 12(3).* 131 - 140.

Jusuf, S. K., Wong, N. H., Hagen, E., Anggoro, R., and Yan, H., 2007. The Influence of land use on the urban heat island in Singapore. *Habitat InternationalJournal.*

Kumar, K. S., Bhaskar, P. U., Padmakumari, K., 2012. Estimation of land surface temperature to study urban heat island effect using LANDSAT ETM+ image. *International Journal of Engineering Science and technology* 4(2). 771 - 778.

Luke, H., 1820. The climate of London: Deduced from Meteorological Observations Made at Different Places in the *Neighbourhood of the Metropolis 2.*

Mallick, J., Kant, Y., Bharath, B. D., 2008. Estimation of land surface temperature over Delhi using LANDSAT 7 ETM+. *Geophysics Union* 3. 131 - 140.

Srivanit, M.; Hokao, K., 2012. Thermal Infrared Remote Sensing for Urban Climate and Environmental Studies: An Application for the City of Bangkok, Thailand. *J. Archit. Plan. Res. Stud. 9*, 83 - 100.

Steffen, W. L., Walker, B. H., Ingram, J. S., and Koch, G. W., 1992, Global change and terrestrial ecosystems: the operational plan. IGBP Report No. 21. International Geosphere - Biosphere Programme. Stockholm.

Tran T. V., Hoang T. L., Le V. T., 2009. Thermal remote sensing method in study on urban surface temperature distribution. *Vietnam Journal of Earth Sciences*, 31(2), 168 - 177.

Treitz, P. M., Howard, P. J., and Gong, P., 1992. Application of satellite and GIS technologies for land-cover and land-use mapping at the rural - urban fringe: a case study. *Photogrammetric Engineering and Remote Sensing* 58. 439 - 448.

Trimble, 2011. eCognition Developer 8.7: User Guide. Trimble Germany GmbH, Trappentreustr. 1, D - 80339 München, Germany.

Trinh L.H., 2014. Studies of land surface temperature distribution using LANDSAT multispectral image. *Vietnam Journal of Earth Sciences* 36(1), 82 - 89.

Valor, E., Caselles, V., 1996. Mapping land surface emissivity from NDVI. Application to European African and South American areas. *Remote Sensing of Environment* 57. 167 - 184.

Waiyamai, K., Songsiri, C., Rakthanmanon T., 2004. Object-Oriented Database Mining: Use of Object Oriented Concepts for Improving Data Classification Technique. *In: Computational Science - ICCS 2004*.

Weng, Q., 1999. A remote sensing-GIS evaluation of urban expansion and its impact on surface temperature in the Zhujiang Delta, China. *International Journal of Remote Sensing* 22(10). 1999 - 2014

Weng, Q., Lu, D., &Schubring, J., 2004. Estimation of land surface temperature-vegetation abundance relationship for urban heat island studies. *Remote Sensing of Environment, 89(4).* 467 - 483.

Yagoub, M. M., Al Bizreh, A. A., 2014, Prediction of Land Cover Change Using Markov and Cellular Automata Models: Case of Al-Ain, UAE, 1992 - 2030, *The Indian Society of Remote Sensing* 42. 665 - 671

Zhang, Z.; Ji, M.; Shu, J.; Deng, Z.; Wu, Y., 2008. Surface Urban Heat Island in Shanghai, China: Examining the Relationship between Land Surface Temperature and Impervious Surface Fractions Derived from Landsat ETM+ imagery. *Int. Arch. Photogramm. Remote Sens. Spat. Inf. Sci., 37. 601 - 606.*